

Contribution of the University of Padova to the EPN Project on Geokinematics

A. CAPORALI and S. BACCINI

Abstract

Time series of coordinates of permanent GPS stations are expected to exhibit a steady, linear trend in response to tectonic forces. This trend is, in fact, observed, but it is accompanied by a variety of signatures, so that the overall spectral properties of the de-trended, zero-mean time series differ from that of a random signal, especially in the medium (~fraction of a year) to long (several years) period. The time series of the coordinates of 30 permanent GPS stations in the Alpine Mediterranean area with time spans from one to five years are presented. The power spectral densities demonstrate that colored noise, mostly flicker phase and -more occasionally- random phase walk noise, can be present at low frequencies, typically below five cycles per year, while at higher frequencies the spectrum tends to a regime of white noise. We use this statistical information to obtain estimates of station velocities and of their uncertainties. Following an approach well known in the analysis of time series of frequency standards, the stability of each time series is computed as a function of time, in the sense of a two-samples Allan variance. The power spectral density of the time series is used to infer the change in the slope, with 1 σ probability, of two consecutive, equal length batches of a given time series, as a function of the length of the batch. The power spectral density of each time series is then converted into the autocorrelation, which measures the statistical dependence of samples of a same process, measured at different times, as a function of the time lag. Taking into account the correct time correlations among the samples, the slope of each time series is estimated by least squares. In all cases, the Allan variances are found to be larger, up to a factor of one hundred, than the variances obtained by least squares under the assumption of pure white noise. Stations with only one year tracking history and a 'pure white noise' formal velocity error of $\sim 0.1 \text{ mm yr}^{-1}$ have a velocity uncertainty, in the sense of Allan variance, of 2 - 3 mm yr^{-1} , which drops to 0.6 - 0.7 mm yr^{-1} with a five years tracking history. For stations whose horizontal coordinates have large (i.e. of the order of up to some millimeter) annual or semi annual oscillations, the autocorrelation has secondary peaks at corresponding lags and the final estimate of the slope can differ of up to 1 mm yr^{-1} , relative to the value which would be obtained assuming uncorrelated samples. We conclude that the reason for the velocity uncertainty estimated by standard least squares being unrealistically small is the neglect of

the cumulative effect of uncorrelated and correlated noise. Contrary to earlier investigations based on limited data sets, we find that the velocity uncertainty does decrease as the time series increases, but this behavior is evident for time series of ~ 3 or more years. We estimate the scale factor to be 10.6 mm for the north component and 6.4 mm for the east component. These values are, as for the velocities, larger than the average formal uncertainties in station coordinates obtained by least squares, but again are probably more realistic, on account of the non random character of noise. The estimates of the velocities and uncertainties of the permanent stations obtained by spectral analysis form the basis for a subsequent investigation of the present-day, large scale strain rate field in the Alpine Mediterranean area, which is implied by these scattered surface displacements.

Introduction

Temporal changes of the coordinates of geodetic stations have formed the basis of important contributions in geophysics and astronomy. In the era of plate tectonics, changes in the coordinates of satellite and VLBI stations have provided direct confirmation of the lithospheric drift implied by time series of magnetic lineations in oceanic crust near areas of active seafloor spreading. Geodesists and geophysicists now face the challenge of understanding quantitatively deformations of the upper part of the crust by correlating in time and space changes of coordinates of networked geodetic stations. Because the non co-seismic horizontal velocity gradients are expected in the order of some mm yr^{-1} for distances of the order of some hundreds of km, each time series must be very carefully examined before attempting to connect temporal changes of coordinates and the state of strain of the underlying crust. In addressing the problem of monument instability in geodetic networks measured with ground techniques, Langbein et al. (1995) and Johnson and Agnew (1995) have pointed out the existence of colored noise in time series. Johnson and Agnew (1995) have emphasized the relevance that temporal correlations have in the measurement of site velocities, and the fact that the variance of the velocity estimates does not necessarily decrease with the increasing number of data points, as it would be expected in the case of uncorrelated data. Langbein and Johnson (1997) have estimated that the seasonal effects are not larger than 3 mm and shown that in small size networks (10 - 20 km) the spectrum of the changes in length of

baselines resembles that of a random phase walk, i.e. proportional to the inverse frequency squared. The time series are relatively short, no more than three years, and the distance measurements are affected by atmospheric gradients along the line of sight, unless two-wavelengths electronic distance meters are used. Large scale networks formed by permanent GPS stations in continuous operations have been addressed by Zhang et al. (1997) and Mao et al. (1999). They showed in a number of examples that the noise spectrum in the coordinate time series consisted of white noise plus flicker phase and/or random phase walk noise, in amounts varying from station to station, and used a Maximum Likelihood Estimator (Langbein and Johnson, 1997) to make estimates of the velocity error. Earlier literature in the subject of noise in time series provides extensive theoretical developments. For example, the fact that the logarithm of the power spectral density is nearly a linear function of the logarithm of the frequency is a property of the time series of phase data delivered by atomic clocks. In some cases the knowledge of the spectral index, i.e. the slope of the power spectral density vs. frequency on a log log basis, is typical of a physical process. For example, shot noise due to the random arrival of particles at a detector in atomic beam devices is described by a random walk of phase, and the associated noise is proportional to the thermal noise and inversely proportional to the square of the quality factor Q of the oscillator. The problem of determining the stability in frequency of an atomic oscillator, as discussed by Allan (1966) or Barnes (1966), has several analogies with the stability of a time series of coordinates of a continuously operating GPS station. In this paper the noise properties of time series of coordinates of permanent GPS stations are examined, with the intention to derive velocities and estimates of their uncertainties. After discussing the data used to construct the time series and to align the network to the conventional terrestrial datum, the spectrum of each coordinate time series is computed and the spectral properties of the low frequency part (frequencies lower than ~ 6 cycles per year) are shown to be consistent with white or flicker phase noise, less frequently with random walk of phase noise, while the high frequency part is very nearly described by white phase noise. The stability of the time series is introduced in the sense of two sample Allan variance and the uncertainties of the velocities -in the sense of slope of time series- are computed accordingly. The knowledge of the power spectral density is also used to compute the autocorrelation of the time series. The non diagonal a priori covariance of the data entering the coordinate time series is constructed on the basis of the autocorrelation function. The velocity estimates are obtained with proper consideration of the time correlated nature of the samples.

Data Reduction

Permanent GPS stations with a tracking history from one to five years are considered. Most of them are part of the European Permanent Network (EPN), and the rest are permanent stations operating on similar quality standards. The data consist of weekly SINEX (Software Independent Exchange Format) files, each containing

adjusted coordinates and the associated variance - covariance matrix, obtained from three different sources (Table 1). The EUREF SINEX files result from a weekly combination done at the Bundesamt fuer Kartographie und Geodaesie (BKG) in Frankfurt on overlapping subnetworks processed by 12 Associate Analysis Centers and forming the European Permanent Network (EPN) (Bruyninx, 2000; Becker et al., 2000). Within the EUREF-EPN activities, each permanent GPS station is processed weekly by three or more EUREF Local Analysis Centers, and the resulting partial SINEX files are submitted to BKG for combination into one, weekly SINEX file for the entire EPN. The additional SINEX files listed in Table 1 include permanent GPS stations which are not part of the EPN but operate on comparable standards. The 'densification' stations used in this work are located in Austria and Italy. The SINEX files of the Austrian stations are computed by the Observatory of Graz, and those of the Italian stations by the University of Padova. The resulting SINEX files are fully compatible with the EUREF SINEX files. EUREF stations common to the three data sets provide the necessary overlap to link the national networks together and to the European Permanent Network. The velocity datum is defined by the ITRF97 velocities of conventionally selected stations. ITRF97 was preferred to the more recent ITRF2000 because virtually all the data reduction, including the reference precise orbits and Earth Orientation Parameters computed by the International GPS Service for Geodynamics (IGS), has been done with reference to the former. On the other hand, the ITRF2000 velocities of the stations in Table 2 differ negligibly from their ITRF97, given the long period of activity. The alignment of the network to ITRF97 is realized by stacking the weekly normal equations and constraining the velocities of such conventionally selected reference stations to their ITRF97 values. These stations, listed in Table 2 together with their assumed ITRF97 horizontal velocities, are part of those normally used to align the European Permanent Network to the ITRF.

Determining a Noise Model for the Time Series of Station Coordinates

The velocities of the individual stations are least squares estimates of the slope of the time series of the coordinates, obtained with the program ADDNEQ, which is part of the Bernese v. 4.2 software (Beutler et al., 1996). Each time series was checked against the logsheet of the station to identify discontinuities related to antenna change or other documented events. As a rule, whenever a change was documented, we tested the discontinuity by solving for new coordinates of that station, while imposing the same velocity. The same procedure was then applied to test undocumented discontinuities, i.e. discontinuities in the coordinate time series without a counterpart in the station logsheet. The results are in Table 3. The time series are modeled by a straight line:

$$x_0(t) = \overline{x_0} + v_0 t + x(t) \quad (1)$$

Most of the data reduction programs estimate by least squares v_0 under the assumption that the residual noise $x(t)$ is white. However Langbein and Johnson (1997) have noted that if the assumed noise model consists only of white noise, the least squares uncertainties in the velocity will tend to underestimate the true uncertainty. Consequently, the uncertainty in implied strain rate - essentially the horizontal gradient of the velocity - would also be scaled over-optimistically. To estimate the best fitting velocity and associated uncertainty with an appropriate noise model, we follow, with modifications to be explained later, the approach of Zhang et al. (1997) and Mao et al. (1999), and compute one-sided noise spectra $S_x(f)$ of the time series for each horizontal coordinate of each station. The spectra tend to be 'flat' (i.e. dominated by white phase noise) in the high frequency part, in the sense of frequencies higher than, say, one cycle every six months, whereas colored (i.e. frequency dependent) noise dominates the low frequency part. This spectral behavior of coordinate time series is common -although on a different scale of frequencies- to other, physically different processes where time series are involved, and is crucial in assessing the *stability* of a time series, that is the property of resisting changes in its rate (Vessot, 1976, ch. 5.4). The stability in phase and frequency of atomic oscillators, for example, has been the subject of detailed studies already in the late 50's and 60's (Barnes, 1966; Spilker, 1977, ch. 12). Borrowing from this well developed approach, the one-sided power spectral density can be approximated by a linear combination of power laws:

$$S_x(f) \approx G_x(f) = \sum_{i=0}^4 \frac{k_i}{f^i} \quad \left[mm^2 yr \right] \quad (2)$$

$i = 0$ White Phase Noise;
 $i = 1$ Flicker Phase Noise;
 $i = 2$ White Frequency Noise
or Random Phase Walk;
 $i = 3$ Flicker Frequency Noise;
 $i = 4$ Random Frequency Walk

where the amplitude of each noise term k_i are estimated by least squares fit of the model in eq. 2 to the spectrum of the de-trended, zero-mean time series of station coordinates. The spectral density is one way of describing the stability. A time domain description is the sample variance of fractional frequency variations. The average velocity over an interval T at time t_k is

$$\overline{y_k} = \frac{x(t_k + T) - x(t_k)}{T} \quad (3)$$

where $k=1,2,\dots$ is the sample number. When N consecutive samples are measured, each of duration T, the variance of the ensemble is known as the Allan variance (Allan, 1966):

$$\langle \mathbf{s}_y^2(N, T) \rangle \equiv \left\langle \frac{1}{N-1} \sum_{n=1}^N \left(\overline{y_n} - \frac{1}{N} \sum_{k=1}^N \overline{y_k} \right)^2 \right\rangle \quad (4)$$

where the brackets denote infinite time average. The Allan variance represents in the time domain another definition of stability in the rate of change of the time series. Because of the existence of processes causing this variance to diverge for large N, Allan (1966) suggested the introduction of the two sample (i.e. N=2) variance :

$$\mathbf{s}_T^2 \equiv \langle \mathbf{s}_y^2(2, T) \rangle = \frac{1}{2} \left\langle \left(\overline{y_{k+1}} - \overline{y_k} \right)^2 \right\rangle \quad (5)$$

This is the variance factor of the probability of a change in rate (eq. 3) from one portion of the time series to the next consecutive, both being of length T.

The one - sided spectrum of a time series of coordinates $S_x(f)$ is related to that of the rate of change $S_y(f)$ of the time series by the equation $S_y(f) = (2\mathbf{p})^2 S_x(f)$. The relation between the two sample Allan variance and the spectral density $S_x(f)$ of the time series is obtained assuming a stationary process (i.e. the time average of the ensemble is not affected by a time translation) and that $\langle y_k \rangle^2 = 0$ (i.e. we are considering departures from the *average* rate of change):

$$\mathbf{s}_T^2 = \frac{1}{T^2} E[x(T) - x(0)]^2 = \frac{2}{T^2} [R_x(0) - R_x(T)] \quad (6)$$

$E[\]$ denotes the expectation value. Hence the variance of the average rate of change depends on the autocorrelation $R_x(t)$ of the coordinate jitter $x(t)$. Using the Wiener - Khinchin Fourier Transform relationship between the one - sided spectral density of a random signal and its autocorrelation function ($\mathbf{w}=2\mathbf{p}f$):

$$R_x(T) = \frac{1}{\mathbf{p}} \int_0^\infty S_x(\mathbf{w}) \cos(\mathbf{w}T) d\mathbf{w} \quad (7)$$

we finally obtain the expression of the two samples Allan variance of a time series with spectrum S_x , as a function of the time T:

$$\mathbf{s}_T^2 = \frac{2}{\mathbf{p}T^2} \int_0^\infty S_x(\mathbf{w})(1 - \cos \mathbf{w}T) d\mathbf{w} = \frac{1}{\mathbf{p}} \int_0^\infty S_y(\mathbf{w}) \frac{\sin^2 \frac{\mathbf{w}T}{2}}{\left(\frac{\mathbf{w}T}{2}\right)^2} d\mathbf{w} \quad (8)$$

For a band limited process with high-frequency f_h it can be shown that the relation between the two sample Allan variance and the components of the spectral density described in (eq. 2) is (Spilker, 1977, Vessot, 1976):

- $i=4$ (random walk of frequency):

$$\mathbf{s}_T^2 = (2\mathbf{p})^2 h_{-4} |T| / 6$$
- $i=3$ (flicker frequency): $\mathbf{s}_T^2 = h_{-3} 2 \ln 2$
- $i=2$ (random walk of phase): $\mathbf{s}_T^2 = \frac{h_{-2}}{2T}$
- $i=1$ (flicker phase):

$$\mathbf{s}_T^2 = \frac{h_{-1}}{(2\mathbf{p}T)^2} \left[\frac{9}{2} + 3 \ln(2\mathbf{p}f_h T) - \ln 2 \right]$$
- $i=0$ (white noise of phase): $\mathbf{s}_T^2 = \frac{3h_0 f_h}{(2\mathbf{p}T)^2}$

The equations above with $i=0$ and $i=2$ have also been obtained by Zhang et al. (1997) (their eq.s A23 and A30, respectively). They are defined by the total time span T and by the highest frequency for which the noise model is valid. Note that for $i=3$ and 4 , the Allan variance is independent of, and respectively increases with the integration time. Once the amplitude h_i of the noise component with the spectral index i has been determined, the uncertainty in the slope of the coordinate time series coming from the corresponding noise process can be estimated, and the total velocity variance (eq. 8) be approximated by the sum of the variances of the individual (white + colored) noise components. This split of the total variance into its potentially several components must however be considered with some caution. Previous studies (Zhang et al. 1997; Mao et al. 1999; Calais, 1999) have shown that the combination of white noise and only one of the colored terms can be considered, for reasons apparently of numerical stability of their Maximum Likelihood Estimator, especially in the presence of relatively short time series and of colored noise.

Estimating station velocities and their uncertainty

The noise model affects not only the variance but also the least squares estimated velocity, in each direction. The vector form of eq. (1) is:

$$X_0 = AZ + \mathbf{e}(t) \quad (9)$$

where X_0 is the time-series of the coordinates, A is the partial derivative matrix of the linear regression, Z is the two-dimensional vector of the unknown intercept and velocity, and $\mathbf{e}(t)$ is the noise vector with elements $x(t)$. The covariance matrix of the residuals of the epoch coordinates relative to the best fitting straight line can be decomposed into the sum of a white noise, nearly (not fully, because of the finite bandwidth) time independent term, and of one or more time - dependent terms, related to colored noise (Langbein and Johnson, 1997). For uncorrelated noise, the covariance of the noise is a diagonal matrix, where each diagonal element is proportional to the variance of the individual estimated coordinate. Time correlated noise will result in a non-

diagonal covariance matrix. The detailed knowledge of the covariance of the noise is necessary for estimating the velocity with the correct noise statistics. We use the normalized autocorrelation $\mathbf{r}_x(T) = R_x(T)/R_x(0)$, T being the lag between any two data points, as an estimate of the covariance of the measurements. By standard least squares formulae:

$$Z \equiv \begin{bmatrix} x_0 \\ v_0 \end{bmatrix} = \left[A^T \mathbf{r}_x A \right]^{-1} A^T \mathbf{r}_x X_0 \quad (10)$$

and the variance of the velocity is :

$$\mathbf{s}_{v_0}^2 = \left[\left[A^T \mathbf{r}_x A \right]^{-1} \right]_{22} \mathbf{s}_0^2 \quad (11)$$

The mean variance \mathbf{s}_0^2 of the coordinate estimates can be obtained *a posteriori* by combining eq.s (8) and (11).

Numerical results

This section shows how the mathematical approach outlined in the previous section has been applied to examine the time series of a number of permanent European stations. Table 4 summarizes the numerical results. For each station we give the total time span in years, the number of data points, each point representing one week of data, the r.m.s. (root mean square) spread of the residuals of the coordinates relative to a best fitting straight line. The following two columns give the noise model appropriate for the low frequency part (< 6 cycles yr^{-1} ; white phase noise always applies to higher frequencies) of the power spectral densities of the coordinate time series, according to the classification in eq.2, for the north and respectively east coordinates. The estimated slopes have been rounded to integers, as we do not see at the moment the need to introduce the concept of fractal (i.e. non integer) spectral index discussed by Zhang et al. (1997). The next two columns specify the uncertainties in the velocity estimates, in the sense of square root of the two samples Allan variance, computed from the spectra with eq.8, via numerical integration. The final two columns give the estimated contribution to the velocity estimates resulting from correlated noise (eq.10) in the north and east time series. Figures 3 to 6 exemplify the numerical results for four stations which we consider typical cases. Part a) of each figure gives the de-trended north and east time series (left column) and the corresponding power spectral densities. These have been computed by means of the PSD function in the program MATLAB v.5 using Hanning windowing over a number of points equal to the total available data, after having padded with zeros the missing data points, to ensure equal intervals. We have, however, verified by direct computation that the slope of the low frequency part is unchanged by using different windowing, e.g. rectangular windowing. Part b) of figures 3-6 shows the autocorrelation functions of the north and east coordinates computed from the corresponding power

spectral densities according to eq. 7, and used in eq. 10 to yield the Δv corrections listed in the last two columns of Table 4. Finally we plot the square root of the two samples Allan variance (eq.8) as a function of the length of the batch T. Thus the knowledge of the power spectral density enables us to predict when, according to the spectral characteristics of the available series, a specified uncertainty in the velocity can be reached. In Figure 7 we make reference to eq. 11 and correlate the root of the Allan variances of the available stations with the square root of the (2,2) element of the variance covariance matrix of the linear regression, to infer *a posteriori* values S_0 of the mean uncertainties of the north and east coordinates which are input to the linear regression. The scatter is considerable but the different slopes indicate that the north coordinates have a typical unit variance (square rooted) S_0 of 10.6 mm, some 80% larger than the corresponding term for the east coordinates, 6.4 mm. Figure 8 shows the correlation between the root of the Allan variance and the inverse square root of the data points in the time series. There is a clear tendency of the square root of the Allan variance to decrease with increasing data points. This fact suggests that white or nearly white (i.e. flicker phase) phase noise processes are dominant in our time series. Had colored noise been important in our time series, then there would have been no guarantee that the uncertainty in the velocity decreases by increasing the number of measurements (Johnson and Agnew, 1995). Finally, we note in Table 4 that the correction to the velocity coming from the inclusion, in the least squares estimator (eq.10), of the temporal correlation of the coordinates is always smaller than the corresponding uncertainty, in the sense of Allan variance. One limiting case is the north component of the velocity of Venice, whose time series are affected by considerable periodic signal, presumably associated with monument noise, as shown in Figure 5. The tendency of long time series to be described by spectral indexes 0 or -1 (white phase or flicker phase noise).

Conclusion

The analysis of time series of geodetic monuments surveyed either by single and dual frequency electronic distance meters, or with GPS, has in the past justified concerns as to the effect of correlated noise in the estimate of the velocity of the monuments. The issue deserves careful examination if strain associated for example to crustal deformation is going to be estimated from surface velocities of the monuments. Our analysis of time series of 30 permanent European GPS stations with time spans ranging from one to five years suggests that when long time series are examined, the deviations from white phase noise, if any, tend to be restricted to flicker phase noise. This evidence is supported by the average spectral index of the low frequency part of the spectrum. We thus confirm earlier findings by Zhang et al. (1997) and Mao et al. (1999), but we find in our examples very little evidence for that random phase walk which motivated Langbein and Johnson (1997) to raise concerns on the possibility of estimating strain rate from velocity measurement of monuments. Our proposed

treatment of uncertainties in the velocities stems from the formalism developed in the 60's for the characterization of the stability of atomic time and frequency standards. We adopt the well known concept of two sample Allan variance intended as the difference in slope of two consecutive, equal length batches of a time series, which is to be expected at the 1σ confidence level, and show that this variance leads to velocity uncertainties larger than those which would be predicted formally, using least squares fit of uncorrelated equal weight data. This also confirms findings by Zhang et al. (1997) and Mao et al. (1999). Our method does not, however, rely on a Maximum Likelihood Estimator, nor does it require the a priori assumptions on the form of the covariance of the data made by Johnson and Agnew (1995). Consistently with our findings of nearly white noise model as dominant noise model for our time series, we find that the Allan variance does decrease with the inverse of the number of samples. Another important element is the negligibly small -with exceptions, such as VENE-correction to the site velocities originating from the time auto-correlation in the elements of a time series, relative to the value obtained assuming uncorrelated data. We therefore conclude that the reason for the uncertainty in the velocity being higher than predicted by standard least squares rests on the uncertainty of the input samples in the time series, which we estimate to be in the order of 10.6 mm for the north and 6.4 mm for the east. If these, we think not unreasonable, values are adopted as mean uncertainty for the input coordinates, then the formal least squares estimate of the velocity uncertainty resembles that obtained by spectral means (Allan variance), when time series of three or more years are considered.

Acknowledgment: this research is supported by a grant of the Ministry of University and Scientific Research and by ASI.

References

- Allan, D.W., *Statistics of atomic frequency standards*, Proc. IEEE, 221-330, 1966.
- Barnes, J.A., *Atomic time keeping and the statistics of precision signal generators*, Proc. IEEE, 207 20, 1966.
- Becker, M., P. Franke, G. Weber, D. Ineichen, and L. Mervart, *EUREF contribution to ITRF2000 and Analysis Coordinator Report for 8/99 - 6/00*, Report on the Symposium of the IAG Subcommission for Europe (EUREF), Tromsø, 22-24 June 2000, Ed. by J.A. Torres and H. Hornik, Veröffentlichungen der Bayerischen Kommission fuer di Internationale Erdmessung der Bayerischen Akademie der Wissenschaften, Astronomisch Geodaetische Arbeiten, Heft n. 61, 31-36, Munich 2000.
- Beutler, G., E. Brockmann, S. Fankhauser, W. Gurtner, J. Johnson, L. Mervart, M. Rothacher, S. Schaer, T. Springer and R. Weber, *Bernese GPS software version 4.0*, ed. by M. Rothacher and L. Mervart, Astronomical Institute of the University of Bern, September 1996, 418 pp.
- Boucher, C., Z. Altamimi and P. Sillard, *The 1997 International Terrestrial Reference Frame (ITRF97)*,

- IERS Technical Note n. 27, Observatoire de Paris, 191 pp., May 1999.
- Bruyninx, C., *Overview of the EUREF permanent network and the network coordination activities*, Report on the Symposium of the IAG Subcommission for Europe (EUREF), Tromsø, 22-24 June 2000, Ed. by J.A. Torres and H. Hornik, Veröffentlichungen der Bayerischen Kommission fuer die Internationale Erdmessung der Bayerischen Akademie der Wissenschaften, Astronomisch Geodaetische Arbeiten, Heft n. 61, 24-30, Munich 2000.
- Calais, E., *Continuous GPS measurements across the Western alps, 1996-1998*, Geophys. J. Int., 138, 221-230, 1999.
- Johnson, H.O. and D.C. Agnew, *Monument motion and measurements of crustal velocities*, Geophys. Res. Lett., 22, 2905-2908, 1995.
- Langbein, J. F. Wyatt, H. Johnson, D. Hamann and P. Zimmer, *Improved stability of deeply anchored geodetic monument for deformation monitoring*, Geophys. Res. Lett., 22, 3533-3536, 1995.
- Langbein, J., and H. Johnson, *Correlated errors in geodetic time series: implications for time dependent deformation*, J. Geophys. Res., 102B1, 591-603, 1997.
- Mao, A., C.G.A. Harrison and T. H. Dixon, *Noise in GPS coordinate time series*, J. Geophys. Res., 104B2, 2797-2816, 1999.
- Spilker, J.J.Jr., *Digital Communications by Satellite*, Information and System Sciences Series, ed. by T. Kailath, Prentice Hall, Englewood Cliffs, New Jersey, 1977, 672 pp.
- Vessot, R.F.C., *Frequency and Time Standards*, in Methods of Experimental Physics, Vol. 12 Part C: Radio Observations, Ed. by M.L. Meeks, 341 pp., Academic Press, New York, 1976.
- Zhang, J., Y. Bock, H. Johnson, P. Fang, S. Williams, J. Genrich, S. Wdowinski, and J. Behr, *Southern California permanent GPS geodetic array: Error analysis of daily position estimates and site velocities*, J. Geophys. Res. 102B8, 18035-18055, 1997.

Table 1: input data sets in the form of SINEX files for three overlapping networks of permanent GPS stations.

Time span (GPS weeks)	# of SINEX data files	total number of stations	Source
860 - 1110	246	133	EUREF Central Bureau
995 - 1110	105	33	University of Padova
1056 - 1099	44	13	Observatory Lustbuehl Graz

Table 2: the stations defining the velocity datum, according to the ITRF97 solution, in mm yr⁻¹.

Station id	#weeks	V _N	V _E
KOSG 13504M003	235	14.59	17.03
VILL 13406M001	230	13.80	18.17
JOZE 12204M001	236	12.94	21.17
METS 10503S011	236	11.36	19.93
ZECK 12351M001	167	7.85	25.68
HOFN 10204M002	169	14.54	9.85

Table 3: documented (Log=Yes) and undocumented (Log=No) discontinuities in time series, their epoch of occurrence [dd.mm.yyyy (GPS week)] and estimated amount of change, in the sense of (value after the break minus value before the break) in N latitude, E longitude and ellipsoidal height. Formal errors are typically less than 0.1 mm. NOTO and NOT1 are physically different monuments, but considered equivalent from the geokinematic point of view.

Station	Log	Break epoch	$\Delta\phi$ (0.001")	$\Delta\lambda$ (0.001")	Δh (mm)
AQUI	No	08.01.2000 (1043)	0.081	0.057	-51.5
BZRG	Yes	29.11.2000 (1090)	-0.042	-0.052	-28.7
MATE	Yes	19.06.1999 (1014)	-0.099	0.305	-4.6
NOTO	No	06.11.1997 (0930)	0.164	0.085	0.5
NOTO	Yes	29.07.1998 (0968)	0.233	0.145	0.2
NOT1	Yes	03.09.2000 (1078)	-	-81.536	125.6
PFAN	Yes	27.07.1999 (1020)	0.172	0.21	-46.5
SBGZ	Yes	29.07.1999 (1020)	0.205	0.239	2.1
SBGZ	Yes	30.10.1999 (1033)	-0.114	0.017	9.8
SRJV	No	05.04.2000 (1056)	-0.324	0.294	7.6
SRJV	No	27.09.2000 (1081)	0.378	-0.445	0.8
TREN	No	28.07.1999 (1020)	0.173	-0.026	58.5
TREN	No	26.04.2000 (1059)	0.4	0.859	118.0
TREN	No	12.07.2000 (1070)	-0.431	-0.808	-0.3
UPAD	Yes	23.12.1997 (0937)	0.038	0.158	-4.3
VEVE	Yes	01.10.1997 (0925)	-0.14	0.057	-17.8
VEVE	Yes	01.02.2001 (1099)	1.84	4.599	72.7
ZIMM	Yes	06.11.1998 (0982)	-0.01	0.19	-23.9

Table 4: statistics of the time series of coordinates of permanent GPS stations: Net indicates the network (E=EPN, D=Densification); span indicates the total extension of the series; #of data is the number of available data points (one estimate of the coordinates is worth one week of data); the following two columns give the root mean square (r.m.s) spread of the residuals of horizontal coordinates, to assess the repeatability of the estimates; following two columns give the estimated noise model for the low frequency part of the spectrum, of the north and respectively east coordinate: with reference to eq. (2) 0= White Phase noise, -1=Flicker Phase noise, -2=White Frequency noise; next two columns give the estimated uncertainty in the velocity, in the sense of two sample Allan variance; last two columns give the correction to the estimated slope of a time series, assuming uncorrelated samples, due to the autocorrelation in time of the samples. All linear units are mm.

Net	Station	span (yr)	# data	r.m.s. north	r.m.s. east	sp.index north	sp.index east	σ_N	σ_E	Δv_N	Δv_E
E	AJAC	1.1	53	2.3	1.64	0	-1	4.81	4.63	0.82	0.02
D	AQUI	1.7	78	1.34	2.01	-2	-1	1.32	1.54	-0.02	-0.69
E	BZRG	2.3	112	2.38	1.66	0	0	1.69	1.71	-0.34	0.02
E	CAGL	4.8	243	2.40	1.90	0	0	0.61	0.7	-0.11	-0.02
D	COSE	1.3	41	1.44	1.63	0	-2	1.34	1.71	0.06	0.11
E	GENO	2.3	113	2.47	1.55	0	0	1.54	1.59	-0.08	0.01
E	GRAS	4.5	217	2.03	1.56	-1	0	0.39	0.36	-0.21	0.05
E	GRAZ	4.8	242	1.63	1.51	0	0	0.57	0.57	-0.06	0.02
E	HFLK	4.8	229	3.53	1.84	0	0	1.31	0.73	-0.35	-0.39
E	LAMP	1.8	88	3.07	2.00	-1	0	5.63	2.46	-0.29	-0.64
E	MARS	2.5	125	2.38	1.49	0	0	1.23	1.21	-0.09	0.03
E	MATE	4.7	240	1.98	2.13	0	0	0.58	0.87	-0.04	0.17
E	MEDI	4.8	241	3.12	3.85	0	0	0.98	1.2	-0.24	-0.12
E	MOPI	4.4	211	1.79	1.91	0	-1	0.65	0.69	-0.24	-0.11
E	NOTO	4.8	227	3.00	2.47	0	0	0.67	0.7	-0.17	0.03
E	OBER	4.2	216	1.87	1.42	-1	0	0.47	0.59	0.04	0.03
E	PFAN	4	198	1.99	2.11	-1	-1	0.54	0.68	-0.02	0.06
D	PRAT	1.2	59	2.96	2.31	0	0	4.81	3.32	0.22	0.09
E	SBGZ	2.2	107	2.33	2.25	-1	0	1.91	2.63	-0.46	0.04
E	SJDV	2.7	134	2.18	1.41	0	0	1.11	1.23	0.01	0.12
E	SRJV	1.1	45	2.11	1.73	0	0	3.94	4.59	0.34	-0.35
E	TORI	2.2	105	2.81	1.59	-1	0	1.67	1.75	-0.69	-0.01
D	TREN	2.1	95	3.62	3.13	-1	-2	2.07	1.35	0.28	0.14
E	UNPG	2.2	106	2.82	1.68	-1	0	1.86	2.05	-0.59	0.02
E	UPAD	4.8	236	2.05	1.95	-1	-1	0.54	0.75	0.04	0.11
E	VENE	4.7	231	2.83	2.37	-1	-1	0.75	0.72	-0.94	-0.16
D	VILH	2.2	90	2.72	3.95	-2	-2	4.07	2.25	-0.33	-0.19
D	VLUC	1.5	67	2.37	3.16	0	-1	3.91	6.75	0.18	-0.14
E	WTZR	4.8	243	1.86	1.66	0	0	0.46	0.65	0.00	0.13
E	ZIMM	4.8	242	1.86	1.44	0	0	0.45	0.54	-0.06	0.15

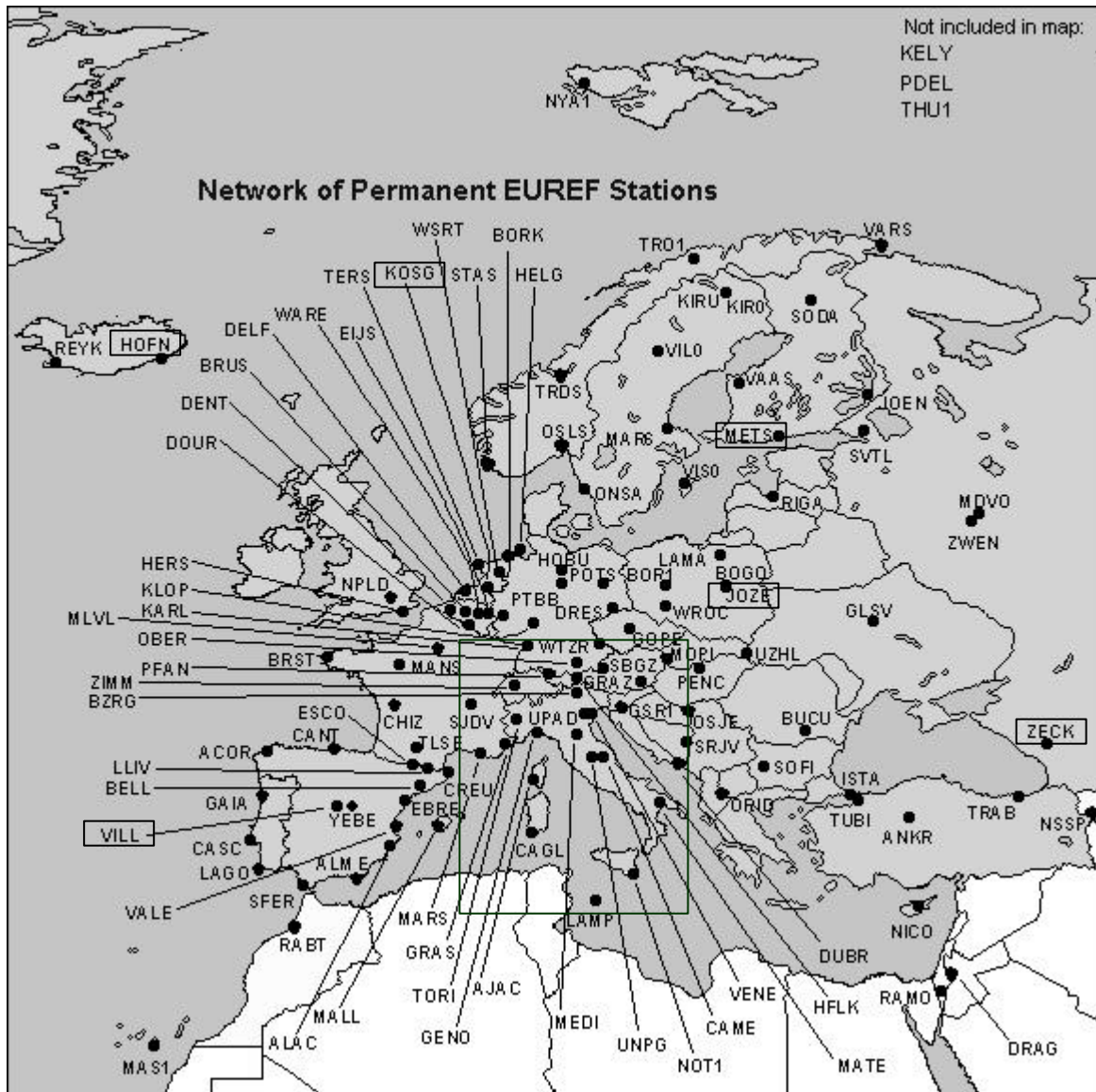


Figure 1: location of the permanent EUREF GPS stations. Solid square borders the study area. For stations inside the box with one or more year of data , velocities have been computed. For the remaining stations, the ITRF97 or EURF 97 values have been assumed. Rectangles identify stations used for the realization of the ITRF97 velocity datum. (From the WEB page of the EBN Central Bureau).

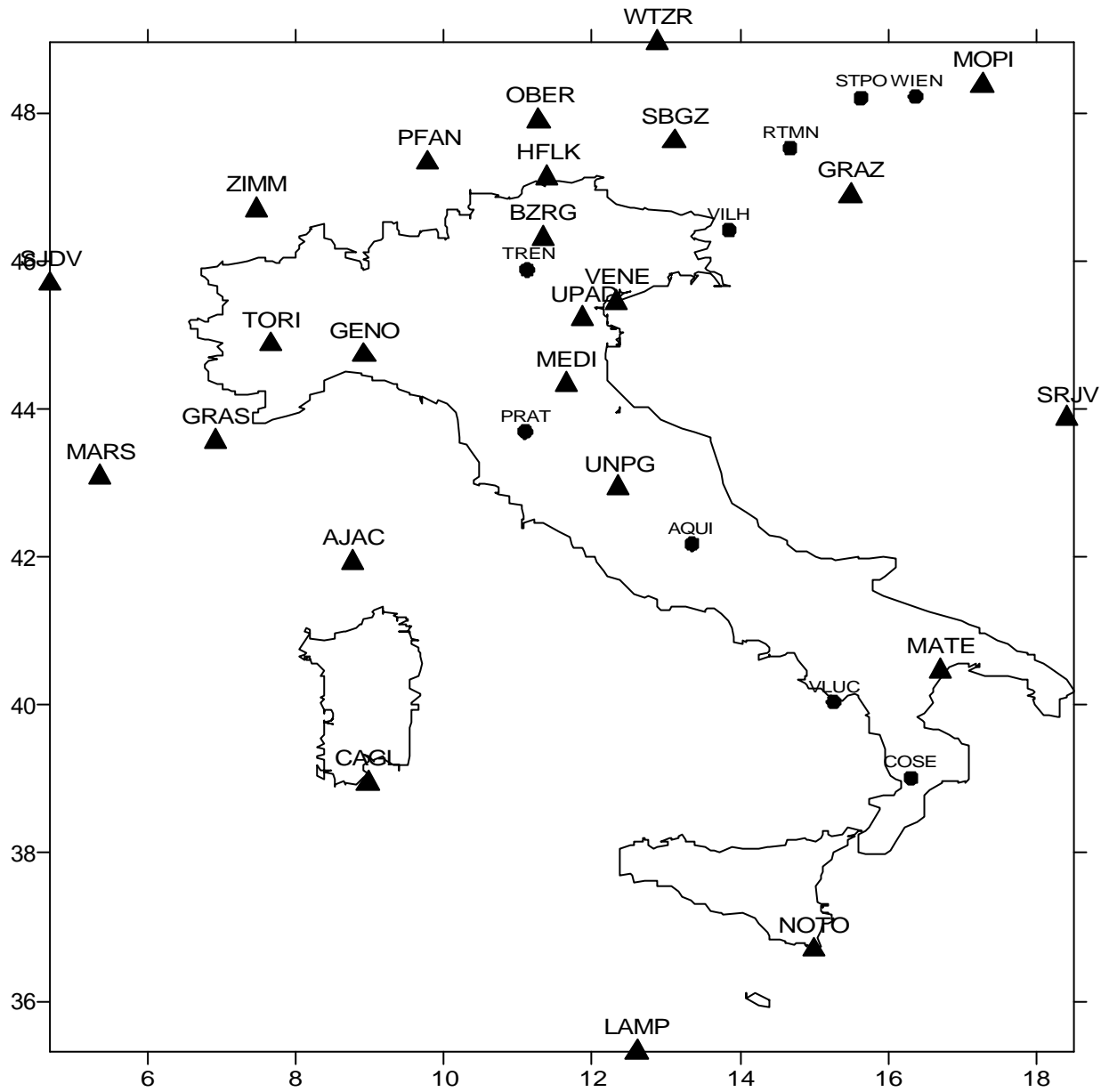


Figure 2: location of the permanent GPS stations analysed in this work. EUREF stations are labelled by a triangle; Densification stations are labelled with a circle.

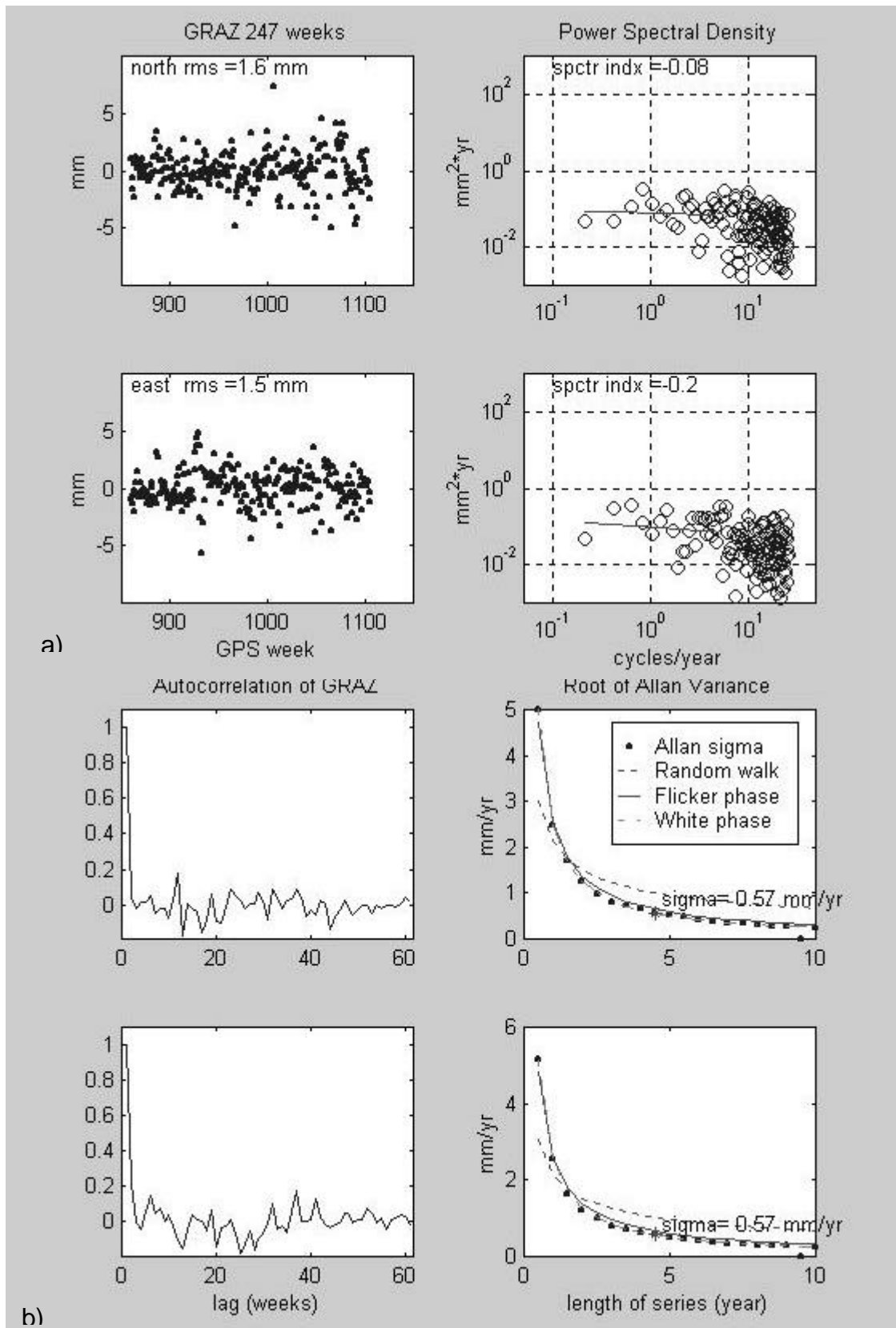


Figure 2: a) left : detrended and zero mean time series of GRAZ for north (above) and east (below) coordinates; right: power spectral density (open circles) and linear interpolation of the low frequency part (below 6 cycles/yr); estimated real value of spectral index is given on top of each figure. b) normalized autocorrelation (left) and plot of the Allan sigma (or square root of two samples Allan variance) for north and east components (right). The dot with a numerical label indicates the estimated current value of the velocity uncertainty. Model curves represent best fitting approximations of the Allan sigma assuming a pure white phase noise (dash dot), flicker phase noise (solid) and random walk noise (dash) models. Note the poor fit provided by the random walk noise model. Flicker phase and white phase noise curves very nearly coincide.

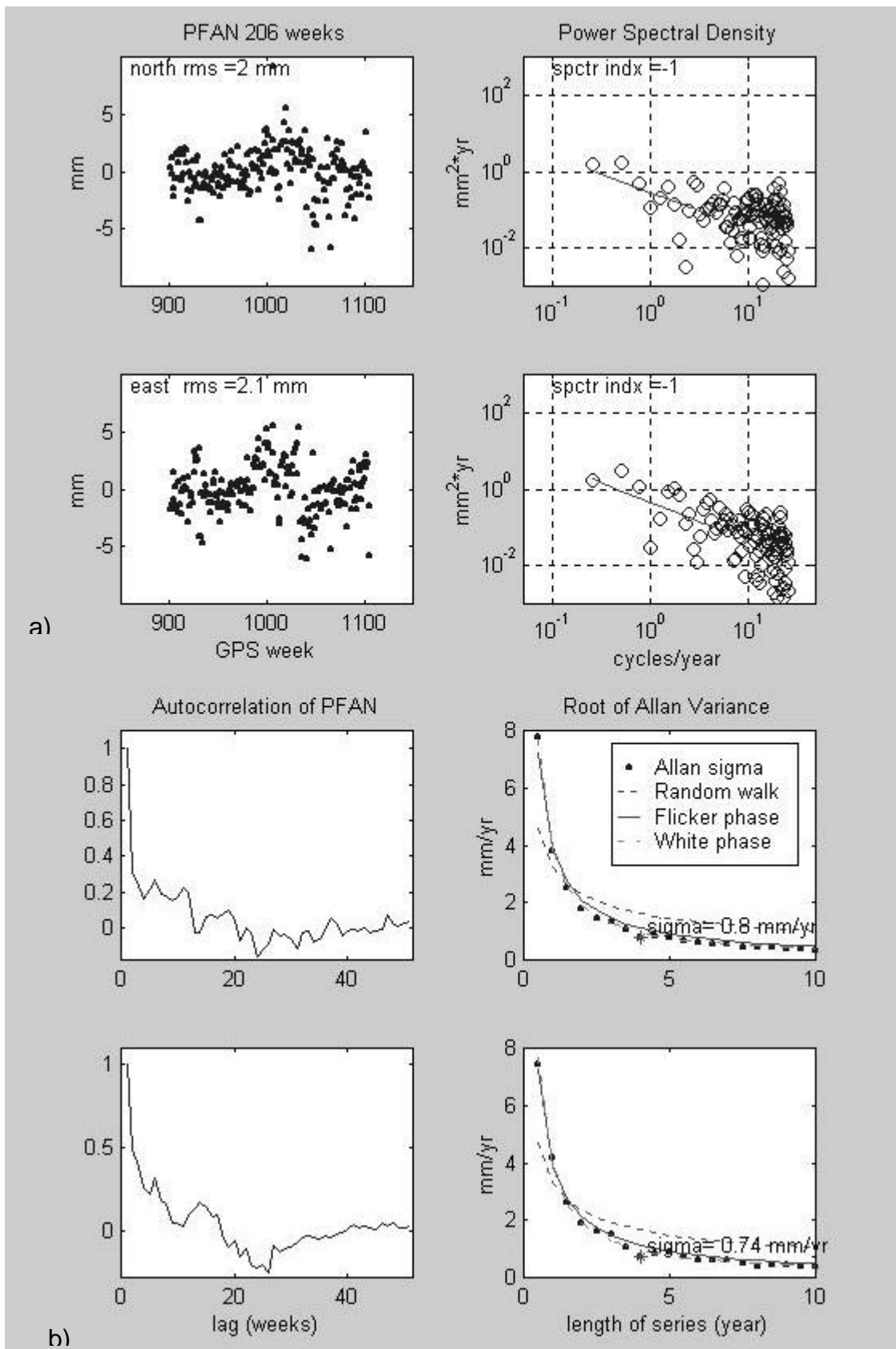


Figure 3: same as figure 3, for the station PFAN.

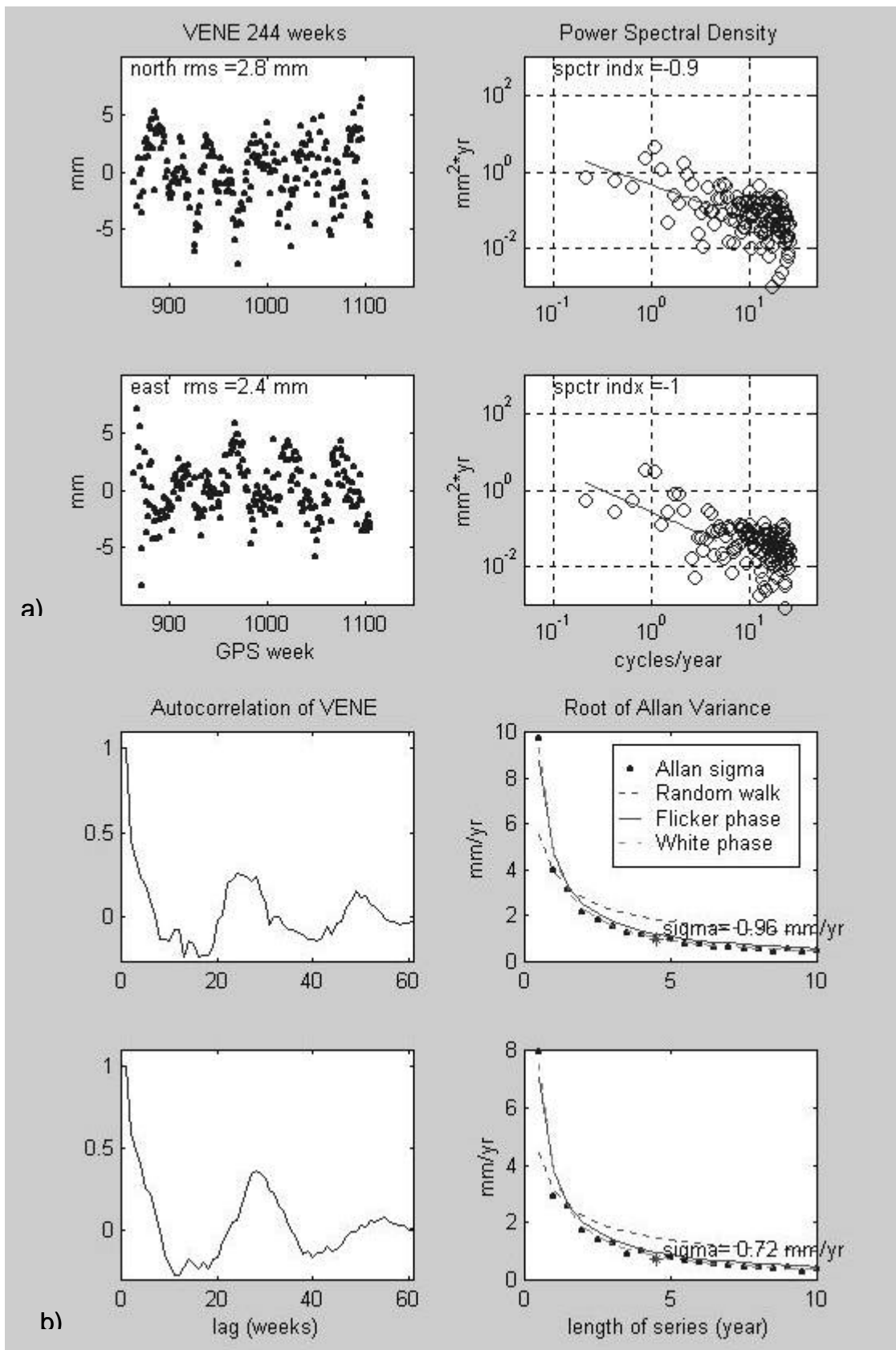


Figure 4: same as figure 3, for the permanent station VENE. Note in this case the large annual and semiannual spectral peaks, perhaps associated with monument instability, causing large autocorrelation peaks at corresponding lags. For this station the correction to the velocity due to the inclusion of the correlation among samples is largest.

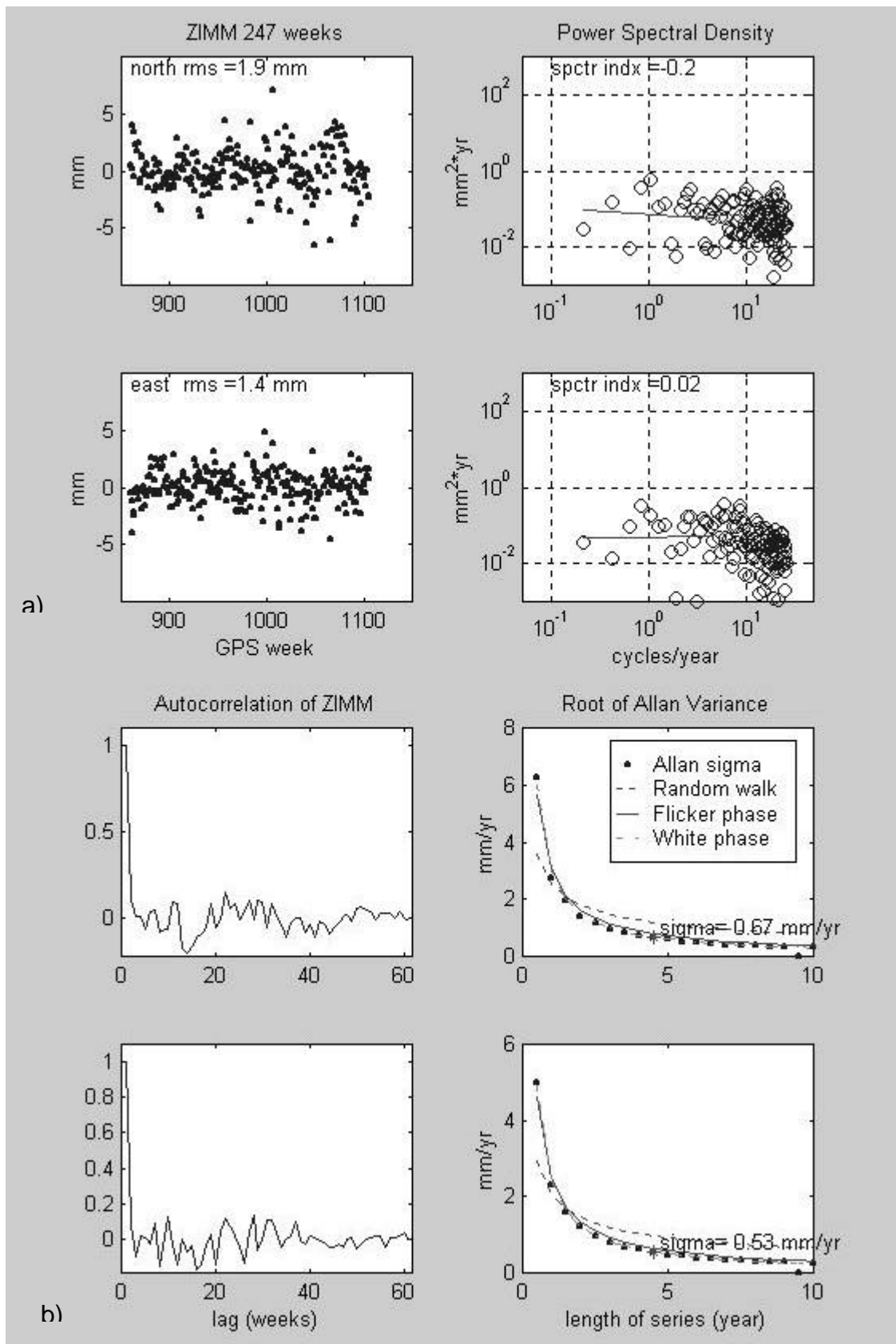


Figure 5: same as figure 3, for the permanent station ZIMM

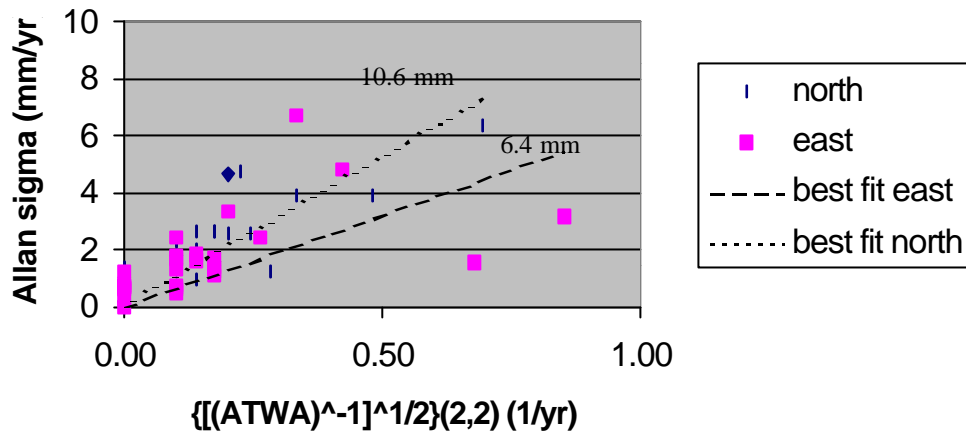


Figure 7: correlation between the Allan velocity uncertainty and the square root of the (2,2) element of the variance covariance matrix in the normal equations of a linear regression, taking into account the time correlation among samples. The correlation coefficients for the east and north time series are an estimate of the corresponding mean uncertainty of the ensemble of samples.

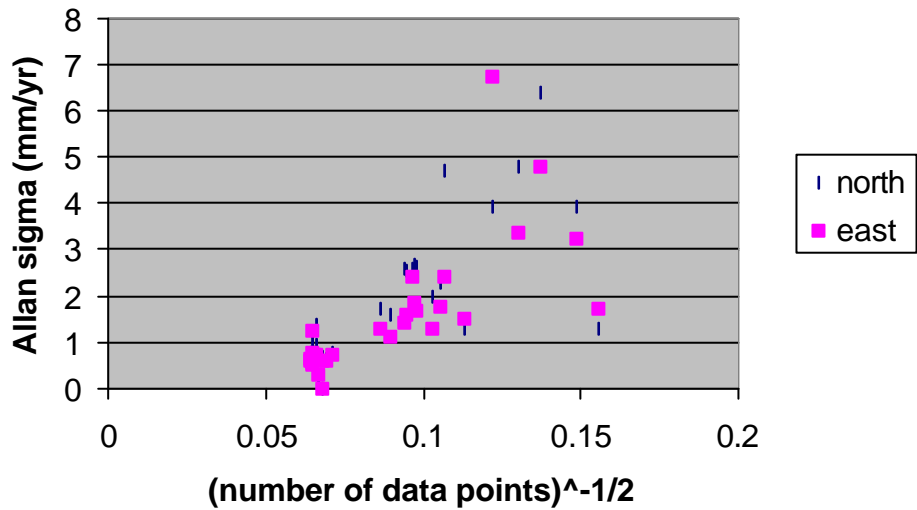


Figure 8: correlation between the Allan velocity uncertainty and the inverse square root of the number of data points in the linear regression. A linear correlation is expected for uncorrelated and equal weight samples.

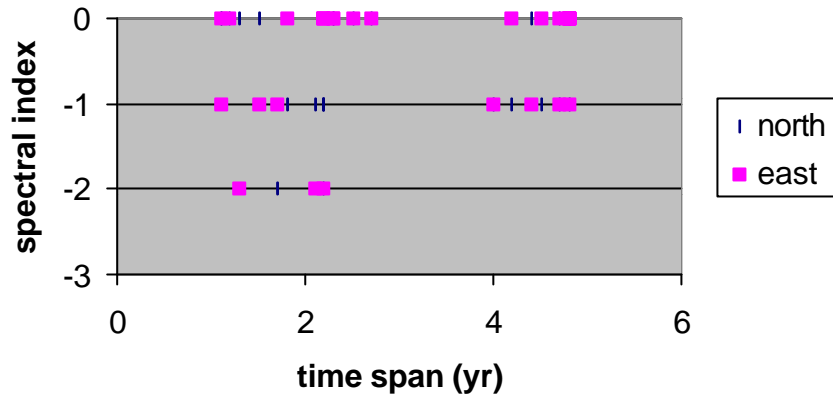


Figure 9: distribution of the spectral index as a function of length of a time series. Random walk ($i=-2$) tends to be unlikely when long time series are analyzed. The average spectral index is -0.4 both for east and north, suggesting that the most probable noise model is white phase noise also at low frequencies.